*atmosphere*

MDPI

*Article*

# Synoptic and Mesoscale Atmospheric Patterns That Triggered the Natural Disasters in the Metropolitan Region of Belo Horizonte, Brazil, in January 2020

**Thaís Aparecida Cortez Pinto [1,2], Enrique Vieira Mattos [1], Michelle Simões Reboita [1,*], Diego Oliveira de Souza [3], Paula S. S. Oda [2,4], Fabrina Bolzan Martins [1], Thiago Souza Biscaro [5] and Glauber Willian de Souza Ferreira [1,2]**

[1] Natural Resources Institute, Federal University of Itajubá (UNIFEI), Itajubá 37500-903, MG, Brazil; thais.cortezp@hotmail.com (T.A.C.P.); enrique@unifei.edu.br (E.V.M.); fabrina@unifei.edu.br (F.B.M.); glauber_ferreira@unifei.edu.br (G.W.d.S.F.)
[2] Post Graduate Program in Environmental and Hydrological Studies, Federal University of Itajubá (UNIFEI), Itajubá 37500-903, MG, Brazil; psayeko@gmail.com
[3] National Center for Natural Disaster Monitoring and Alerts (CEMADEN), São José dos Campos 12247-016, SP, Brazil; diego.souza@cemaden.gov.br
[4] Post Graduate Program in Earth System Sciences, National Institute for Space Research (INPE), São José dos Campos 12227-900, SP, Brazil
[5] Center for Weather Forecasting and Climate Studies (CPTEC), National Institute for Space Research (INPE), Cachoeira Paulista 12630-000, SP, Brazil; thiago.biscaro@inpe.br
* Correspondence: reboita@unifei.edu.br

**Abstract:** Between 23 and 25 January 2020, the Metropolitan Region of Belo Horizonte (MRBH) in Brazil experienced 32 natural disasters, which affected 90,000 people, resulted in 13 fatalities, and caused economic damages of approximately USD 250 million. This study aims to describe the synoptic and mesoscale conditions that triggered these natural disasters in the MRBH and the physical properties of the associated clouds and precipitation. To achieve this, we analyzed data from various sources, including natural disaster records from the National Center for Monitoring and Early Warning of Natural Disasters (CEMADEN), GOES-16 satellite imagery, soil moisture data from the Soil Moisture Active Passive (SMAP) satellite mission, ERA5 reanalysis, reflectivity from weather radar, and lightning data from the Lightning Location System. The South Atlantic Convergence Zone, coupled with a low-pressure system off the southeast coast of Brazil, was the predominant synoptic pattern responsible for creating favorable conditions for precipitation during the studied period. Clouds and precipitating cells, with cloud-top temperatures below −65 °C, over several days contributed to the high precipitation volumes and lightning activity. Prolonged rainfall, with a maximum of 240 mm day$^{-1}$ and 48 mm h$^{-1}$, combined with the region's soil characteristics, enhanced water infiltration and was critical in triggering and intensifying natural disasters. These findings highlight the importance of monitoring atmospheric conditions in conjunction with soil moisture over an extended period to provide additional information for mitigating the impacts of natural disasters.

**Keywords:** natural disasters; synoptic analysis; mesoscale features; thunderstorms; Minas Gerais state

check for updates

Academic Editors: Marcio Cataldi and Franciele Zanandrea

Received: 20 December 2024
Revised: 11 January 2025
Accepted: 15 January 2025
Published: 18 January 2025

**Citation:** Pinto, T.A.C.; Mattos, E.V.; Reboita, M.S.; Souza, D.O.d.; Oda, P.S.S.; Martins, F.B.; Biscaro, T.S.; Ferreira, G.W.d.S. Synoptic and Mesoscale Atmospheric Patterns That Triggered the Natural Disasters in the Metropolitan Region of Belo Horizonte, Brazil, in January 2020. *Atmosphere* **2025**, *16*, 102. https://doi.org/10.3390/atmos16010102



## 1. Introduction

Under global warming, extreme weather events are expected to become more frequent, following a trend already observed [1]. Climate change has quintupled the occurrence of natural disasters [1], as they can contribute both to increasing the frequency of occurrence of extreme natural events [2] and to increasing socio-environmental vulnerability [3,4].

The unregulated growth of urban areas has significantly disrupted the hydrological cycle, mainly by altering surface drainage capacity. Consequently, the frequency and intensity of natural disasters, such as floods, landslides, and flash floods, have increased, resulting in severe socioeconomic challenges and heightened risks to human life [5]. According to the Brazilian Atlas of Natural Disasters [6], between 1991 and 2012, approximately 126.9 million people were affected by natural disasters in Brazil. Of these, 21% were impacted by flash floods, 12% by floodings, 1.79% by landslides, and 1.32% by urban waterlogging (here, also called by flood). Flash floods were the leading cause of fatalities from 1991 to 2012, accounting for 58.15% of deaths, followed by landslides at 15.60% [6]. At this point, it is important to provide a brief distinction between the terms “flood” (urban waterlogging), “flooding”, and “flash flooding”. Here, the term “flood” is used synonymously with urban waterlogging and refers to precipitation accumulation in urban areas due to infrastructure issues. “Flooding” emphasizes the ongoing process or condition of being inundated with water, typically occurring when a water body overflows. Meanwhile, “flash flood” describes a sudden and rapid water overflow caused by intense rainfall or dam failures, usually occurring within minutes to hours and often with destructive force.

The southeastern region of Brazil, composed of four states (Minas Gerais, Rio de Janeiro, São Paulo, and Espírito Santo), has the highest number of deaths per capita associated with natural disasters (28 deaths per million inhabitants), exceeding the national average of 18 deaths per million inhabitants [6]. According to the National Confederation of Municipalities (CNM), Minas Gerais state (Figure 1) recorded the highest number of natural disasters in Brazil over the past decade, totaling approximately 8095 events, including flash floods, floods, and landslides [7]. Many of these events are closely linked to extreme precipitation during the austral summer [6]. The southeastern region of Brazil is significantly influenced by the South American Monsoon System, which concentrates accumulated rainfall during the austral summer months (December–February; DJF) [8]. However, it is essential to note that the region’s climate is also shaped by factors such as latitude, altitude, continentality, and the influence of the South Atlantic Subtropical Anticyclone (SASA) [8].

The history of natural disasters in the Minas Gerais state is long-standing. For instance, in 1979, Minas Gerais experienced one of its worst floodings, which isolated 37 municipalities and caused 246 deaths after 35 consecutive days of rain. In 1991, heavy rains impacted Belo Horizonte (the capital of the state), the Zona da Mata region, and the southern part of the state, resulting in 42 deaths. The following year, rainfall over 30 consecutive days affected 47 municipalities, leading to 33 deaths and leaving 33,000 people homeless [9]. According to the Brazilian Integrated System of Information on Natural Disasters (S2iD), between 2003 and 2016, a State of Public Calamity and a State of Emergency were declared 2677 times in 2056 different municipalities in Minas Gerais [10]. More recently, in January 2020, the media reported an extreme precipitation event that triggered flooding and flash floods [11]. According to Dalagnol et al. [12], this natural disaster primarily affected the Metropolitan Region of Belo Horizonte (MRBH), impacting more than 90,000 people and resulting in economic losses estimated at approximately USD 250 million.

The recurrence of natural disasters in the MRBH requires effective monitoring of risk areas, environmental education, and efficient state public policies. Regarding monitoring natural disasters, the performance of civil defense and data availability from rainfall stations, satellites, radars, radiosondes, and numerical weather forecasting models have proven to be a fundamental strategy [13]. However, few studies have comprehensively analyzed these data to investigate the underlying causes and consequences of disaster occurrences in this critical region of Brazil. Therefore, the aim of this study is to describe the synoptic and mesoscale conditions that triggered the natural disasters in the MRBH between 23 and 25 January 2020, which affected more than 90,000 people, as well as the physical properties of the associated clouds and precipitation.

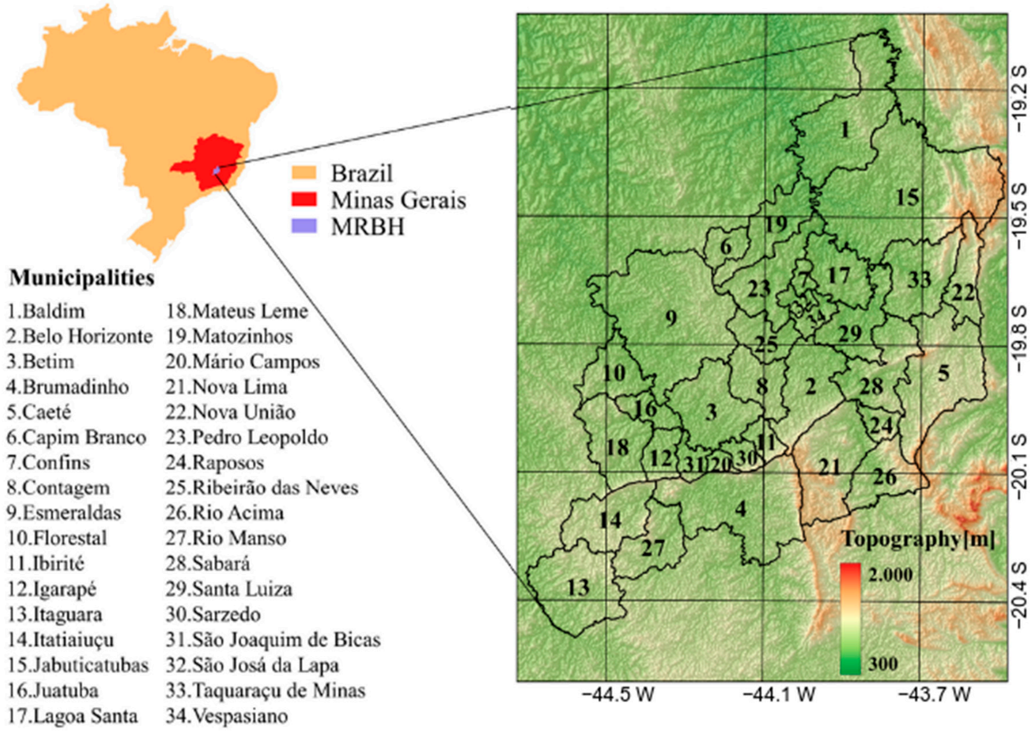


**Figure 1.** Location and topography (meters) of the municipalities comprising the Metropolitan Region of Belo Horizonte (MRBH) in the Minas Gerais state (left side panel), Brazil.

## 2. Materials and Methods

This study focused on the MRBH (Figure 1) and the natural disasters that occurred between 23 and 25 January 2020. The MRBH comprising 34 municipalities and data from different sources were used in this study: records of natural disasters, precipitation from rain gauges, reanalysis data, satellite images, weather radar, and lightning information, as summarized in Figure 2 and described as follows.

### *2.1. Natural Disasters, Precipitation Data, and Analysis*

For the identification of natural disasters that occurred in the Minas Gerais state between 23 and 25 January 2020, we used the database of the National Center for Monitoring and Early Warning of Natural Disasters (CEMADEN). This database provides the date, location (latitude and longitude), type of disaster (flood, flooding, flash flood, and landslide), and the number of people affected. The primary objective of analyzing natural disaster occurrence data was to identify the most predominant disasters during the study period. For this purpose, a histogram of relative frequency was made. In addition, these data allow us to identify the spatiotemporal patterns of natural disasters in the MRBH.

The precipitation rate plays a pivotal role in the occurrence of natural disasters. In this context, precipitation data from rain gauges provide reliable estimates with high temporal resolution. The main objective was to evaluate precipitation intensity in January 2020 within the MRBH. For this analysis, data from 19 rain gauges operated by CEMADEN, located within 5 km or less of the natural disasters, were utilized (Figure 3). These data have a temporal frequency of 10 min and are available at http://www2.cemaden.gov.br/mapainterativo/# (accessed on 10 July 2024). To determine the day of January 2020 and the hour of the day in which the most precipitation occurred, the analyses for each pluviometer were separated into two steps: (i) daily precipitation for January 2020 and (ii) hourly precipitation on 24 January 2020.

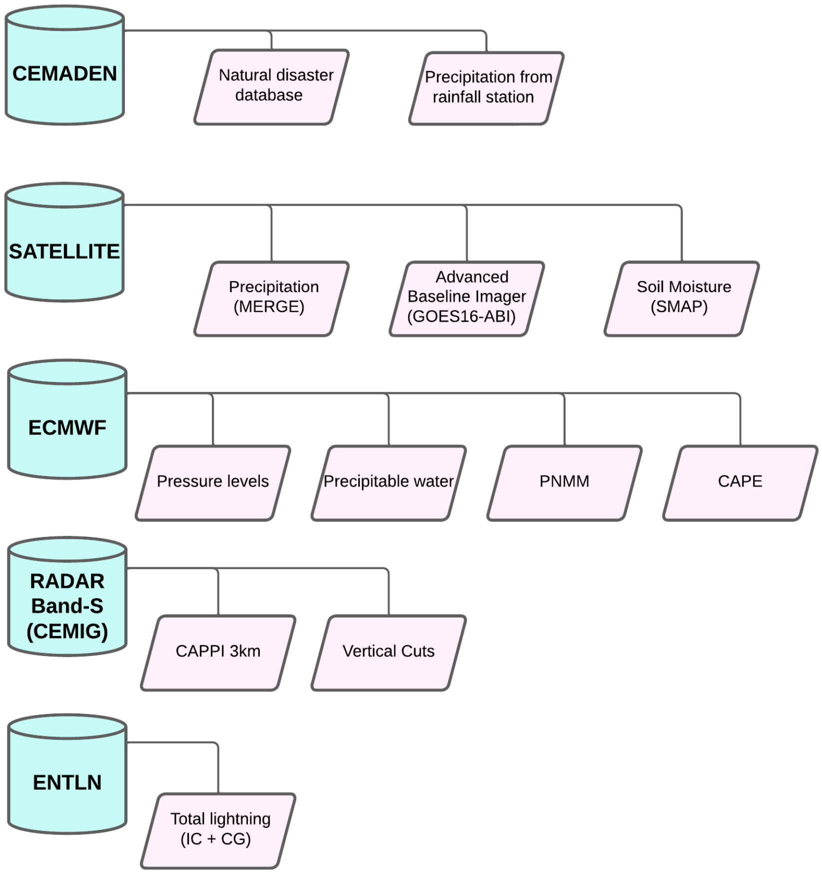


**Figure 2.** Data flowchart used in this study. PNMM, IC, and CG means the mean sea-level pressure, intracloud, and cloud-to-ground lightning, respectively.

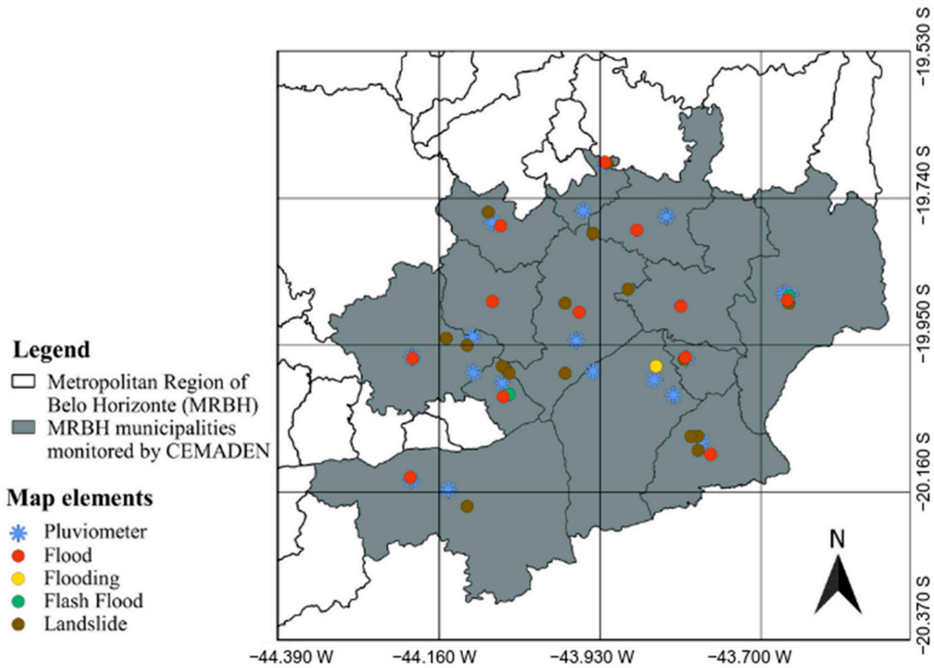


**Figure 3.** Spatial distribution of natural disasters and the location of pluviometers for the event that occurred between 23 and 25 January 2020, at MRBH. Disasters are represented by colored circles:

red-Flood, yellow-Flooding, green-Flash Flood, and brown-Landslide. Blue stars represent the pluviometer's location. The region highlighted in gray represents the municipalities monitored by CEMADEN, and in white, the municipalities covered by the MRBH. See the introduction section for the definition of flood, flooding, and flash flood.

### *2.2. Meteorological Satellite, Radar Data, and Analysis*

We use satellite and radar data to describe the mesoscale patterns associated with clouds and precipitation from 23 to 25 January 2020. Precipitation estimates from satellites indicate spatial distribution in large regions and are widely used for monitoring natural disasters [14]. Precipitation from the MERGE product was used to assess the spatial distribution of rainfall in the MRBH. MERGE combines precipitation estimates by the satellites from the Global Precipitation Measuring (GPM) Integrated Multi-satellite Retrievals for GPM (IMERG) with precipitation measurements from pluviometers [15]. MERGE has a spatial resolution of 0.1° (longitude × latitude), accumulated precipitation in hourly, daily, and monthly scales, and is available at http://ftp.cptec.inpe.br/modelos/tempo/MERGE/GPM/ (accessed on 10 July 2024).

Monitoring cloud-top properties is a good way to obtain information on the intensity of thunderstorms [16]. For example, clouds with lower cloud-top temperatures are typically area-related to stronger updraft conditions and efficient ice formation. To assess the spatial distribution of the clouds that triggered the natural disasters, brightness temperature information from the Geostationary Operational Environmental-16 (GOES-16) satellite, made available at INPE, was used (http://ftp.cptec.inpe.br/goes/goes16/retangular/, accessed on 8 April 2024). Brightness temperatures of the 10.3 µm infrared channel (Ch13) from the Advanced Baseline Imager (ABI) sensor were used, with a spatial resolution of 2 km and a temporal resolution of 10 min. The ABI sensor and the infrared channel were chosen due to their importance for evaluating clouds and cloud-top characteristics such as size and temperature. For this purpose, maps of infrared brightness temperature from 23 to 25 January 2020 were made.

In addition to precipitation, soil moisture is an important factor in contributing to the trigger of natural disasters [17]. To test this hypothesis, we evaluated the spatial–temporal behavior of soil moisture before, during, and after natural disaster occurrences. For this analysis, surface soil moisture (mm) data from Soil Moisture Active Passive (SMAP), a National Aeronautics and Space Administration (NASA) satellite product that spans the globe [18], were used. The data have a spatial resolution of 10 km and were processed through Google Earth Engine (https://developers.google.com/earth-engine/datasets/catalog/NASA_USDA_HSL_SMAP10KM_soil_moisture#bands, accessed on 20 September 2021). The dataset represents an integration between soil moisture native observations from SMAP into the modified two-layer Palmer model using a 1-D Ensemble Kalman Filter (EnKF) data assimilation approach. SMAP employs estimates from microwave measurements provided by a microwave radiometer at 1.41 GHz and a Synthetic Aperture Radar (SAR) at 1.26 GHz. We have used the SMAP dataset rather than the model dataset (e.g., ERA5) due to the strong correlation between microwave measurements and soil conditions. Several works have utilized satellite-based soil moisture estimates to analyze natural disasters, yielding promising results [19,20]. In this work, a spatial analysis was performed with the SMAP for 24 January 2020, and a time series from December 2019 to February 2020, was inspected to elucidate the soil moisture behavior before, during, and after the occurrence of natural disasters.

Weather radar data were also used to analyze the storm's vertical structure. The radar is located in Belo Horizonte city (19.94° S and 44.43° W) and is operated by the Minas Gerais Energy Company (CEMIG). The weather radar is located at 128.0 m altitude, operating with a temporal resolution of 8 min. Constant Altitude Plan Position Indicators (CAPPIs) were produced, with a horizontal and vertical spatial resolution of 1 km, ranging from 3 to 15 km in height. Reflectivity CAPPI images at a height of 3 km were plotted from 23 January to 25 January at 12 different times to track the storm. In addition, since 24 January was the day with the highest precipitation accumulation, vertical cross-sections of the storm were derived using the CAPPIs from 3 to 15 km height. The vertical cross-sections are commonly used to visualize a two-dimensional section of the storm in its interior [17,21,22].

### *2.3. Reanalysis and Synoptic Analysis*

ERA5 reanalysis from the European Center for Medium-Range Weather Forecasts (ECMWF) [23] provided the atmospheric variables used in this study. Reanalysis combines historical observations and outputs of numerical models [24]. The data used have a spatial resolution of 25 km and hourly frequency. The variables obtained at pressure levels (950, 850, 700, 600, 550, 500, 300, 250, and 200 hPa) were: horizontal wind components, mass divergence, air temperature, specific humidity, and vertical velocity. In addition, we also used precipitable water, mean sea-level pressure (MSLP), and Available Convective Potential Energy (CAPE) from 23 to 25 January 2020. Through the data mentioned, the following synoptic fields (maps) were produced: (i) wind intensity at 250 hPa (representative of upper-level jets), thickness at 500–1000 hPa (representative of the horizontal temperature gradients), mass divergence at 250 hPa (it triggers upward movement in the atmosphere column), and MSLP (it allows to identify high and low-pressure systems); (ii) precipitable water and runoff 850 hPa; (iii) moisture convergence at 850 hPa, wind vectors at 850 hPa, and negative vertical velocity (omega) at 500 hPa (representative of upward movement); and (iv) vertical wind shear between 1000 and 500 hPa, which is an approximation for the layers at 0 and 6 km in height. Additionally, synoptic charts from the Center for Weather Forecasting and Climate Studies (CPTEC) of the National Institute for Space Research (INPE) were used. These charts are for three atmospheric layers: (i) near-surface, (ii) middle (500 hPa), and (iii) upper-levels (250 hPa).

### *2.4. Characterization of Spatial Distribution of Lightning*

Clouds that produce lightning are related to intense thunderstorms, which can produce higher precipitation rates. In addition, a higher lightning rate (Lightning Jump) typically precedes severe weather events (strong winds, hail on the surface, and tornadoes) [25]. In this way, the spatial distribution of lightning for 23, 24, and 25 January 2020 was analyzed. For this purpose, data from the Earth Networks Total Lightning Network (ENTLN) of the Earth Networks were used. This network has approximately 70 sensors covering the south and southeast regions and parts of Brazil's midwest and northeast regions. The data used refer to return strokes and comprise the information of date and time of occurrence; it is worth mentioning that throughout the text, the word lightning was used to refer to return strokes. Previous studies indicate that total lightning data—representing the sum of intracloud (IC) and cloud-to-ground (CG) lightning—is a better proxy for convection intensity than CG lightning alone. Accordingly, total lightning data for 23, 24, and 25 January 2020, were interpolated onto a grid with a 4 km spatial resolution. Daily total lightning density maps were generated, representing the number of lightning events (IC plus CG) per square kilometer per day.

## 3. Results and Discussion

### *3.1. Overview of Natural Disasters and Associated Impacts*

The heavy precipitation events took place between 23 and 25 January 2020, affecting several municipalities in the MRBH, totaling 32 occurrences of natural disasters. The most recurrent typology was landslides, with 17 records, and floods, with 12 records (Figure 4).

In some places, more than one type of phenomenon was recorded (Figure 3). According to Dalagnol et al. [12], these natural disasters affected more than 90 thousand people, causing 13 deaths. The economic losses reached approximately USD 240 million (the dollar exchange rate in January 2020 was BRL 4.09). The press recorded some landslides and flooding in photos, as shown in Figure 5. The roads were inundated with water and mud, rendering passage impassable for vehicles and pedestrians.

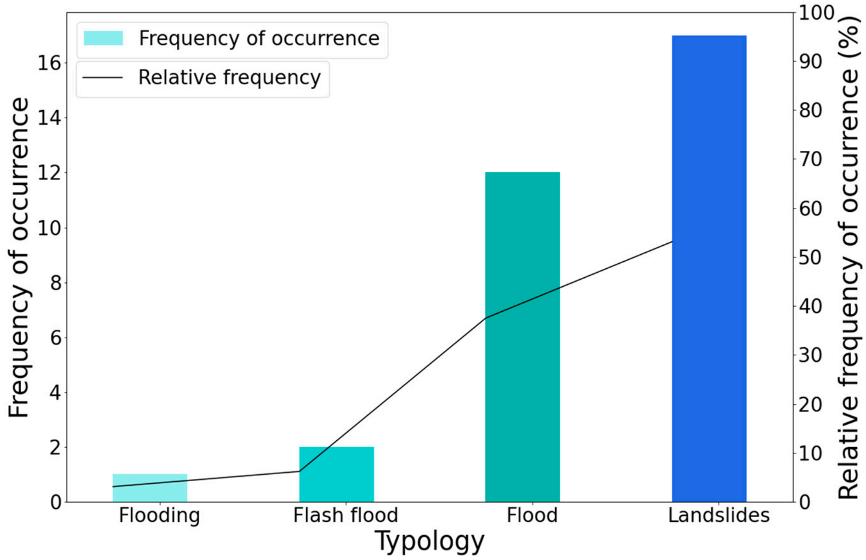


**Figure 4.** Distribution of types (flooding, flash flood, flood, and landslides) of natural disasters in the MRBH occurred between 23 and 25 January 2020 for the municipalities monitored by CEMADEN.

**Figure 5.** Photograph records of the consequences of the natural disasters' events in Belo Horizonte on 24 January 2020. Source: G1—Photos: Reproduction/TV Globo (https://g1.globo.com/mg/minas-gerais/noticia/2020/01/24/chuva-forte-provoca-alagamento-na-pampulha-em-belo-horizonte.ghtml, accessed on 16 January 2022).

Figure 6 shows the accumulated daily precipitation in January 2020 from the pluviometric stations located in the MRBH. January begins with heavy rainfall in several municipalities (Figure 6a–d), with values close to 100 mm day$^{-1}$. In addition, some cities registered intense precipitation on 17 January (more than 100 mm day$^{-1}$), for example: Brumadinho (230 mm day$^{-1}$ in the pluviometer of Alberto F., Figure 6b) and Raposos (140 mm day$^{-1}$ in the pluviometer of Água L., Figure 6c). On the following days, even with less intensity, the rain remains constant, as in the case of Caeté (Figure 6b) and Nova Lima (Figure 6c). On the other hand, on 23 January, the rain covered all cities, with high rainfall rates (above 50 mm day$^{-1}$). However, the precipitation peak occurred on 24 January, mainly in Nova Lima (Vale do S., Figure 6c), with a volume greater than 200 mm. According to Parizzi et al. [26], it can rain up to 350 mm in January in Belo Horizonte, so the precipitation recorded on the 24th (122.98 mm) can be considered intense, as this value represents 35% of what was expected for the month. In addition, the highest number of landslides in the MRBH was observed on this day.

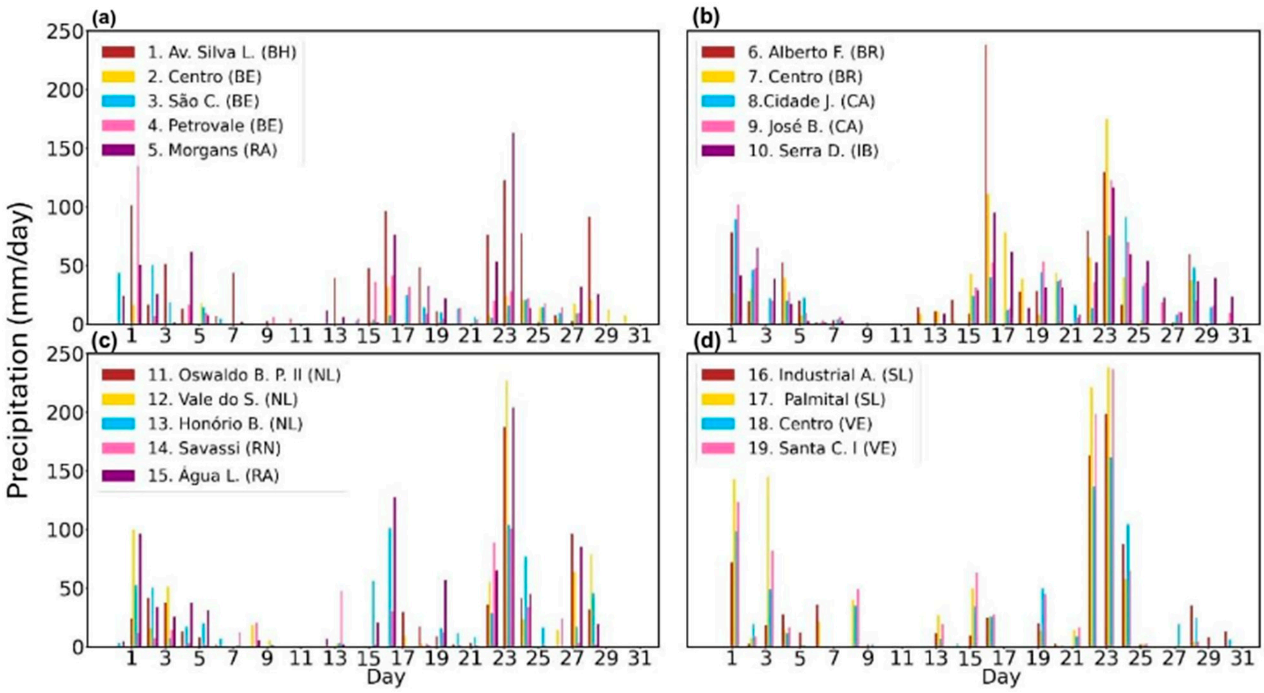


**Figure 6.** Accumulated daily precipitation (mm day$^{-1}$) in the MRBH in January 2020 with data from pluviometers provided by CEMADEN for the cities: (**a**) Belo Horizonte (BH), Betim (BE), Rio Acima (RA), (**b**) Brumadinho (BR), Caeté (CA), Ibirité (IB), (**c**) Nova Lima (NL), Ribeirão das Neves (RN), Raposos (RA) and (**d**) Santa Luzia (SL), Vespasiano (VE).

Satellite information is an additional component and essential for a better understanding of the rainfall spatial distribution in this region. Figure 7 shows the spatial distribution of the accumulated daily precipitation from the MERGE product. It is possible to observe that the rain is distributed throughout the Minas Gerais state on the 24th and 25th (Figure 7b,c). However, it is in the MRBH that the largest accumulations occur (~170 mm day$^{-1}$). Hence, this result converges with the data measured in the rainfall station. However, despite the focus of this study being the MRBH, other regions of Minas Gerais also experienced intense precipitation.

Regarding the accumulated hourly precipitation for 24 January 2020 (Figure 8), it can be observed that there was a record (close to 50 mm h$^{-1}$) of rainfall at certain times. In some cities, the rain occurred constantly during the day, as in the case of Ibirité (Serra D.) and Caeté (Cidade J. and José B.) (Figure 8b). On the other hand, it is noted that in Belo Horizonte (Av. Silva L., Figure 8a), the highest volume of rain was concentrated in the early morning hours, totaling more than 40 mm in 5 h. This observation aligns with the time of occurrences recorded by the media [11] (Figure 5). In addition, note that the precipitation peak (48 mm h$^{-1}$) at the beginning of the day in several cities, such as Nova Lima (Oswaldo B. P., Vale do S., and Honório B., Figure 8c), is possible. The distribution by type of natural disasters in the MRBH shows a higher frequency of landslides (53.1%), followed by floods (37.5%) (Figure 4). The reason for the highest occurrences of landslides may be the intense precipitation from January 23 to 25. However, the preceding rains may have contributed to intensifying the natural disasters.

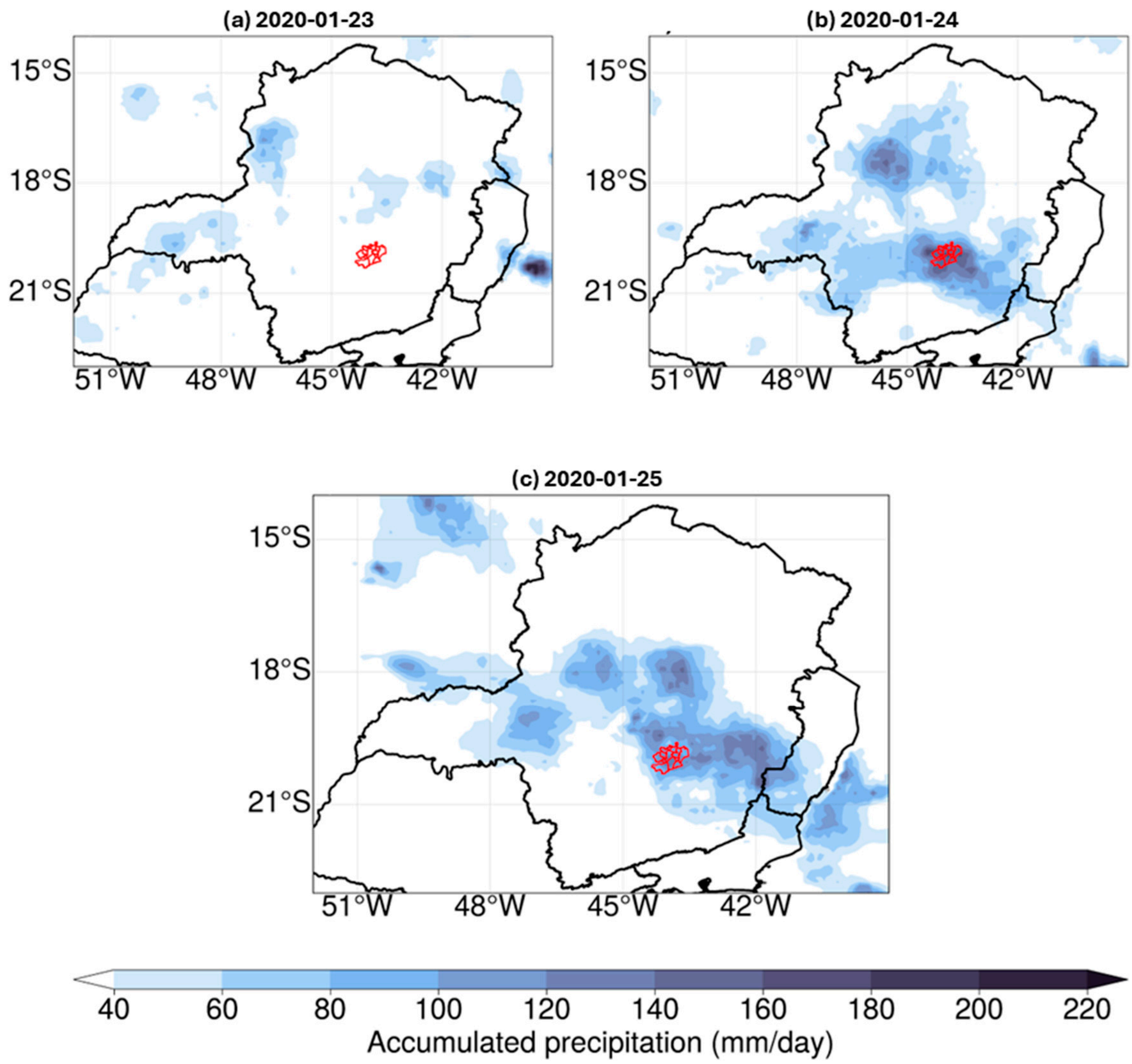


**Figure 7.** Accumulated daily rainfall (mm day$^{-1}$) from the MERGE product for the days: (**a**) 23, (**b**) 24, and (**c**) 25 January 2020. The red line represents the MRBH.

In addition to the topography and precipitation rates, another factor influencing the frequency and magnitude of natural disasters is the use and occupation of risk areas. The occupation of risk areas is especially problematic in episodes of extreme rainfall when precipitation is greater than the soil's capacity to retain water, exceeding the saturation level and causing landslides and floods. In this context, soil moisture content, when near to (or above) the available capacity of soil water, aggravates these occurrences [27,28]. For example, the SMAP products show that in most parts of the Minas Gerais state, soil moisture (Figure 9a) values were close to 25 mm, representing almost the maximum soil moisture value the SMAP product could estimate. Mendes et al. [29] found that the critical soil moisture content values for triggering landslides are close to soil saturation. Figure 9b helps to understand the temporal behavior of soil moisture content. Note that on 24 January, when there was a higher occurrence of mass movements, soil moisture was above the average for the period (represented by the gray line). This result is expected since it was on this day that the peak of precipitation occurred in most municipalities in the MRBH (Figure 6). However, what draws attention to this figure is that in December, the soil moisture values were already above the average for the summer period (gray line). In this way, the precipitation that preceded the event may also have contributed to the numerous occurrences of landslides in several places between the 23rd and the 25th of January. On the 24th, for example, more than 100 mm were registered in Belo Horizonte, a municipality hit by landslides. As demonstrated in the study by Barbosa [30], heavy and less intense but prolonged rains favor this type of phenomenon.

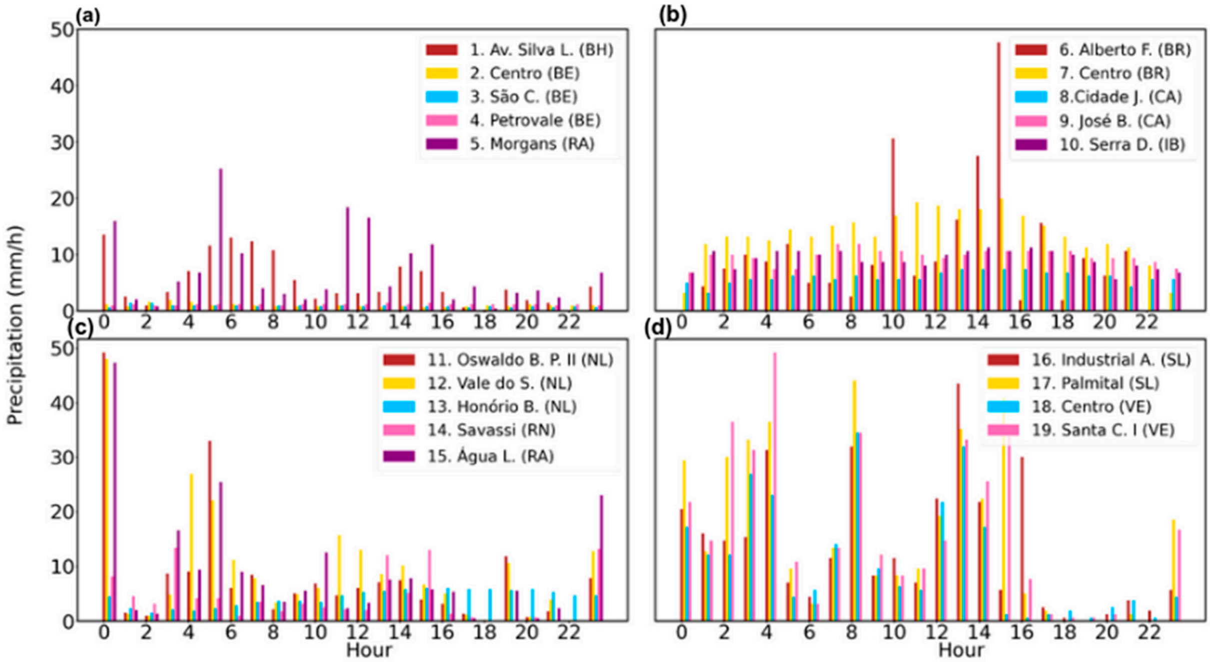


**Figure 8.** Accumulated hourly rainfall (mm $h^{-1}$) in the MRBH on 24 January 2020 for the cities: (**a**) Belo Horizonte (BH), Betim (BE), Rio Acima (RA), (**b**) Brumadinho (BR), Caeté (CA), Ibirité (IB), (**c**) Nova Lima (NL), Ribeirão das Neves (RN), Raposos (RA) and (**d**) Santa Luzia (SL), Vespasiano (VE).

### 3.2. Synoptic Patterns

Figure 10 shows the near-surface, mid-level, and upper-level atmospheric conditions between 23 and 25 January 2020. During these three days, at upper levels, the Bolivian High is displaced southwest from its climatological position. There is a trough between southeastern Brazil and the South Atlantic Ocean, and downstream of this system, an amplified ridge is present (Figure 10a–c). Eastward of the ridge, the upper-level cyclonic vortex appears within the figure's domain only on 25 January (Figure 10c). At mid-levels (Figure 10d–f), the most prominent features are the ridge over Chile, which is also a signature of the Bolivian High, and the trough between the continent and the Atlantic Ocean. Throughout the period, the mid-level trough axis crosses the western portion of southeastern Brazil, leaving most of Minas Gerais on its eastern side. Therefore, Minas Gerais is under favorable conditions for upward movement in the atmospheric column and, consequently, cloud development. At the near-surface (Figure 10g–i), under the interface between the trough and the ridge over the Atlantic Ocean at mid-levels, the South Atlantic Convergence Zone (SACZ) is indicated in green. Its oceanic branch is connected to a subtropical cyclone (absence of fronts linked to the low-pressure center) called Kurumi by the Brazilian Navy, which underwent an extratropical phase on January 25. The described circulation pattern in Figure 10 is typical of SACZ episodes [31]. The SACZ is generally welldefined when there is a cold front or a cyclone near the coast [32], as these low-pressure systems help create a horizontal pressure gradient that channels the continental flow toward southeastern Brazil.

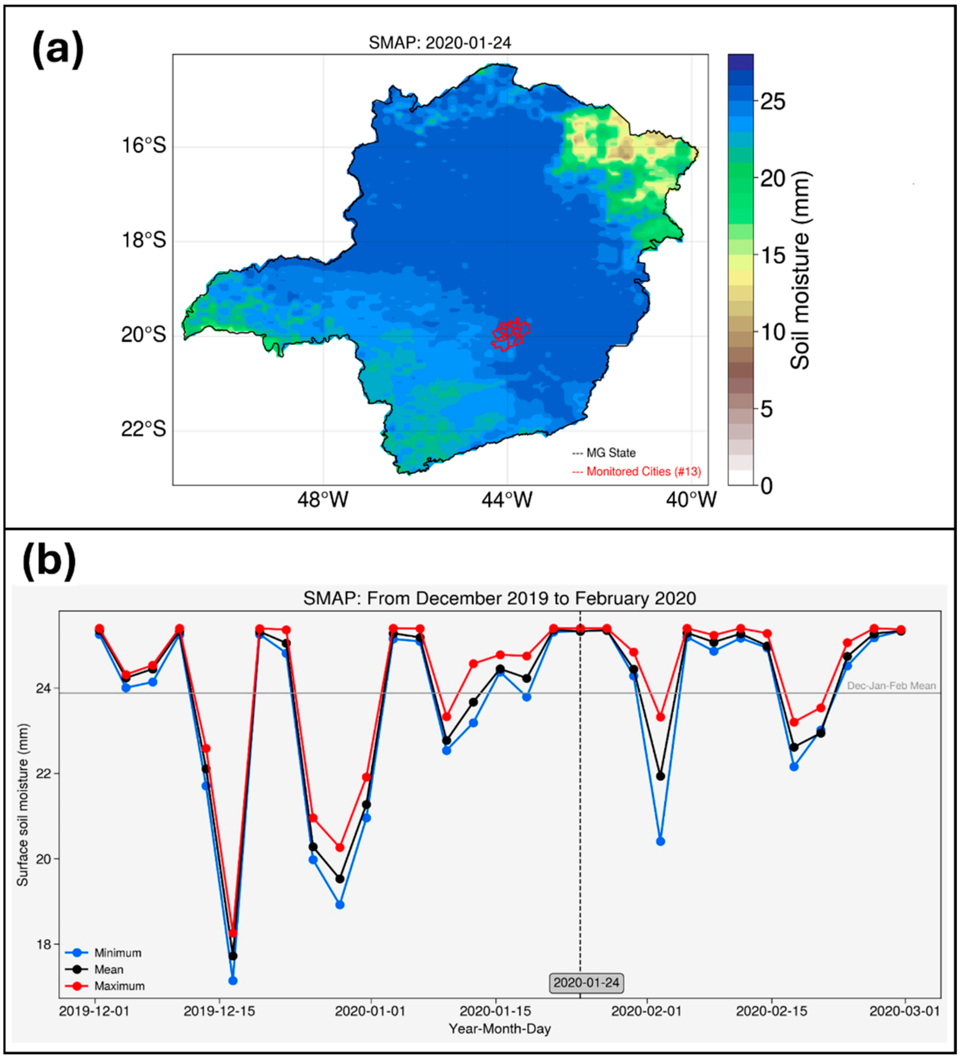


**Figure 9.** (**a**) Soil moisture (mm) in the Minas Gerais state on 24 January 2020, from SMAP product. The red line represents the MRBH. (**b**) Time series from December 2019 to February 2020 of soil moisture in MRBH from SMAP, which are represented by the minimum (blue), mean (black), and maximum (red) values inside the region. The gray horizontal line represents the mean soil moisture content value between December 2019 and February 2020.

After an extensive analysis of different atmospheric fields, the indication of the SACZ is provided in the near-surface chart (Figure 10g–i). Some of these fields are shown in Figure 11 (in this study, we focused only on the Minas Gerais state). Along with the upper-level winds, it is important to consider the mass divergence, which was intense on 24 January around the MRBH (indicated by the red line in Figure 11(1b)). Under this area of divergence, there is an area of convergence at 850 hPa, resulting from the meeting of northwesterly and southeasterly winds (Figure 11(2b)). The northwest winds transport warm, moist air from the Amazon to Minas Gerais, while southern winds bring humidity from the Atlantic Ocean due to low pressure on the Brazilian coast. This moist air can be observed through the precipitable water (Figure 11(2b)). The combination of these variables triggers upward movement. Indeed, Figure 11(3) shows the upward motion at 500 hPa around the MRBH. The upward movements are also influenced by surface warming during the austral summer. In summary, the combination of the described patterns led to the development of a persistent band of clouds and precipitation from southern Amazonia to the Atlantic Ocean named the SACZ which is the primary precipitation system in southeastern Brazil during the summer [33].

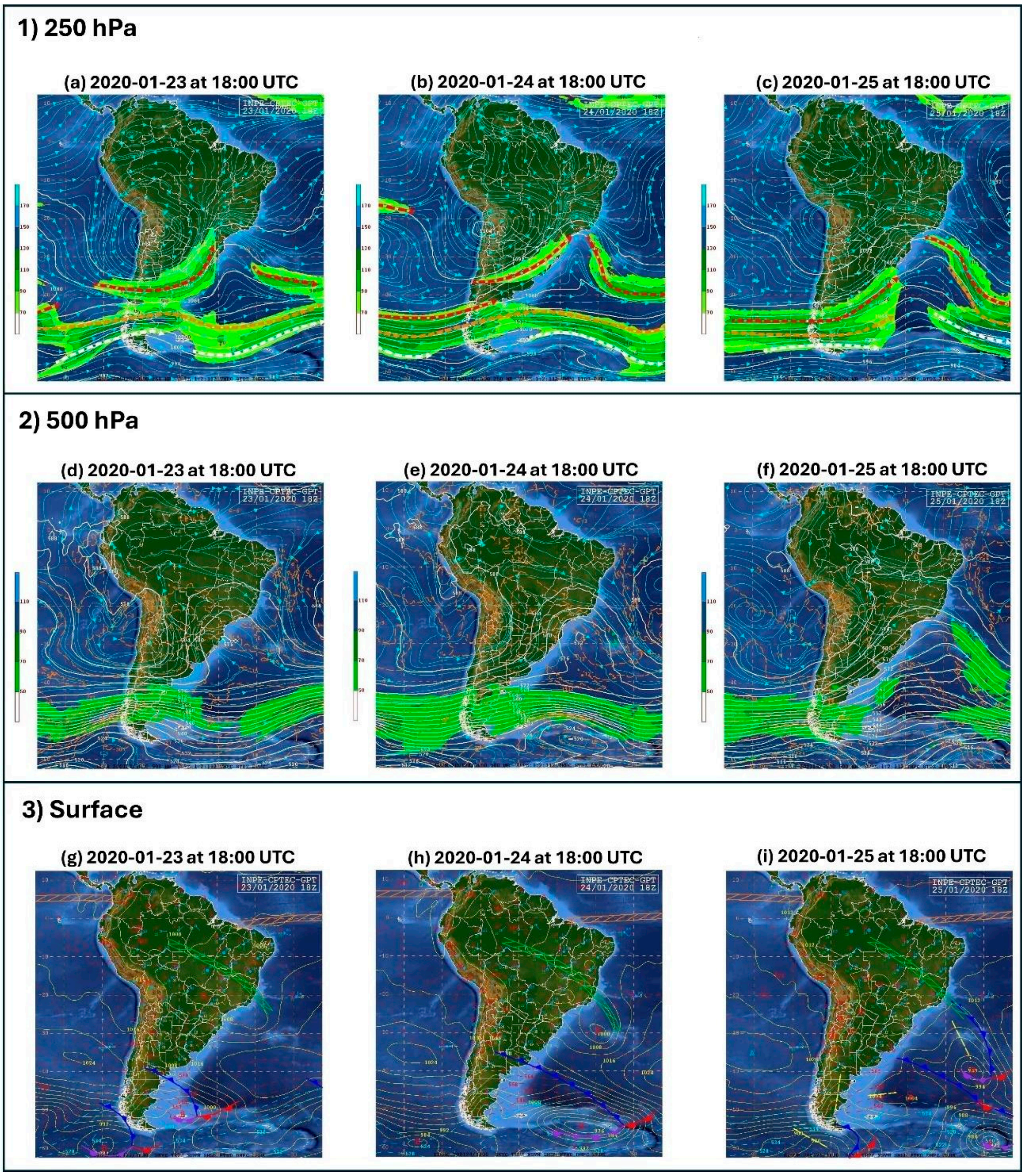


**Figure 10.** Synoptic charts at (**a**–**c**) 250 hPa, (**d**–**f**), 500 hPa, and (**g**–**i**) near-surface for 23, 24, and 25 January 2020 at 18:00 UTC. In (**a**–**f**), streamlines are indicated in cyan, wind intensity (knots) in shaded, and geopotential height in white lines. In (**a**–**c**), the upper-level jets' core is highlighted in dashed lines. In (**g**–**i**), MSLP is indicated by yellow lines, and the thickness of 500–1000 hPa by dashed lines; this level also shows the atmospheric systems: Intertropical Convergence Zone (orange), SACZ (green), cold fronts (blue), warm fronts (red) and occluded fronts (purple). Source: CPTEC/INPE.

Once the ingredients for cloud formation are present, the clouds must regenerate continuously. The vertical wind shear magnitude between 0 and 6 km (represented by the levels of 1000 and 500 hPa) is a reliable indicator of the dynamic environmental conditions supporting thunderstorm development and maintenance [34]. Figure 11(4) shows that the vertical wind shear varied from 9 to 16 m $s^{-1}$ around the MRBH. Shear values exceeding 5–10 m $s^{-1}$ indicate favorable conditions for the formation of thunderstorms [34–36]. These shear values, combined with the warm and moist air predominant in the region were fundamental to forming clouds and precipitation.

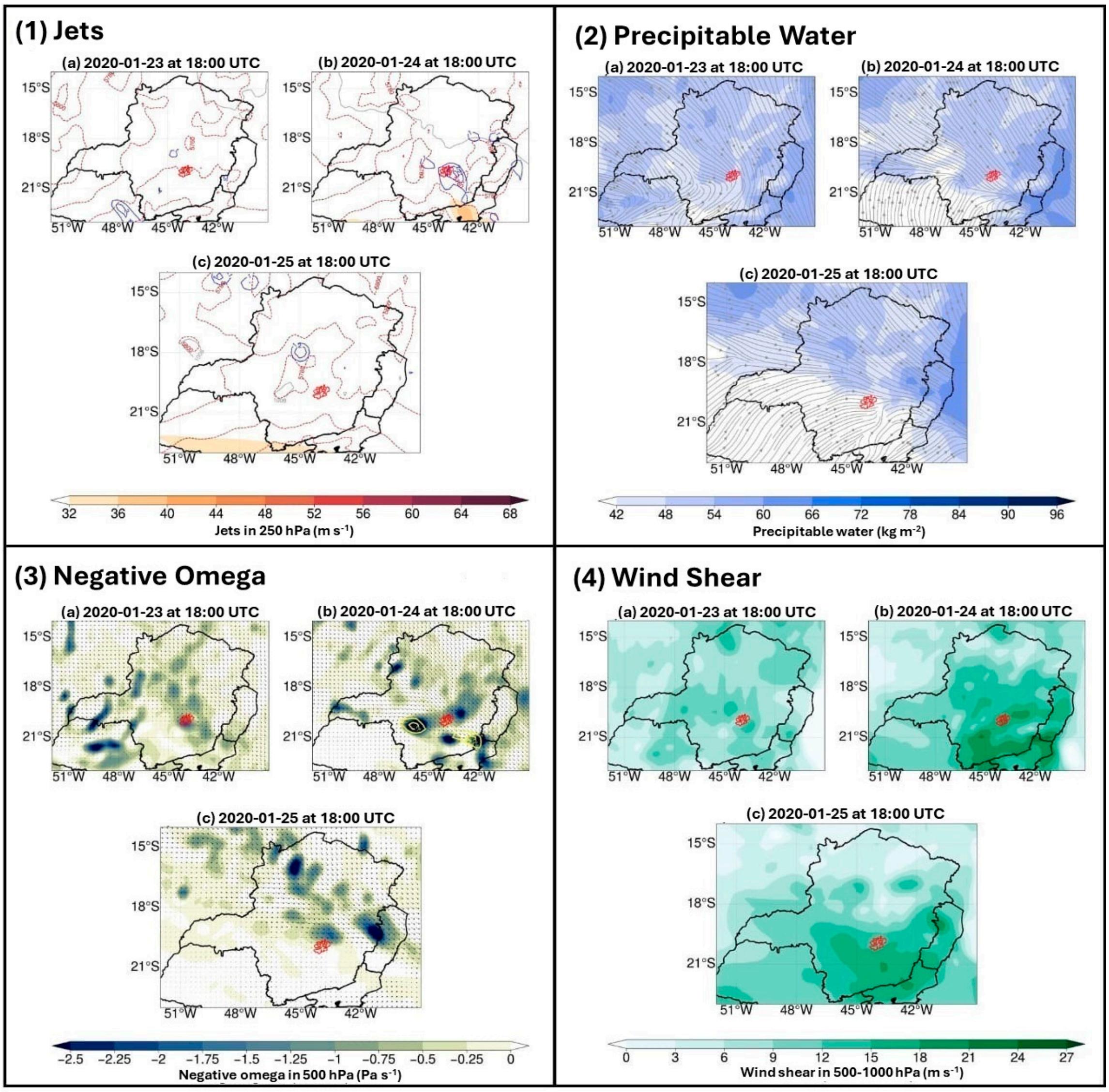


**Figure 11.** Atmospheric fields at 18:00 UTC on (**a**) 23, (**b**) 24, and (**c**) 25 January 2020. (**1**) Wind intensity at 250 hPa higher 30 m $s^{-1}$ s (shaded), thickness 500–1000 hPa (m; red dotted lines), mass divergence at 250 hPa ($\times 10^{-5}$ $s^{-1}$; blue line), and mean sea level pressure (MSLP, gray lines). (**2**) Precipitable water (shaded) and streamlines at 850 hPa. (**3**) Convergence (yellow lines) and winds (vectors) at 850 hPa and vertical velocity at 500 hPa (Pa $s^{-1}$, negative values in shaded). (**4**) Vertical wind shear 500–1000 hPa (m $s^{-1}$). In all panels, the red line represents the MRBH.

### *3.3. Physical Characteristics of the Thunderstorms*

Figure 12b shows that, at the beginning of 23 January, the state of Minas Gerais was already covered with extensive cloud cover. However, during the afternoon of the 23rd (Figure 12d) and continuing into the 24th (Figure 12e–h), the convective cloud cluster initially concentrated over the Goiás state (Figure 12a), shifted and remained over Minas Gerais, particularly over the MRBH (indicated on the map by red lines). The cloud-top temperature over the study region on this day was approximately −60 °C, indicating deep vertical development and the presence of multiple Cumulonimbus clouds. Note that the cloud band is well-organized in the northwest–southeast direction the following day (Figure 12i–l). As discussed earlier, this cloud band was characterized by the formation of the SACZ over the study region. Additionally, on 25 January, between 00:00 UTC (24 January, 21:00 local time) and 06:00 UTC (25 January, 03:00 local time), intense convective cores persisted, with cloud-top temperatures near −75 °C, including over the MRBH. After this period, the region remained cloudy, likely dominated by stratiform clouds.

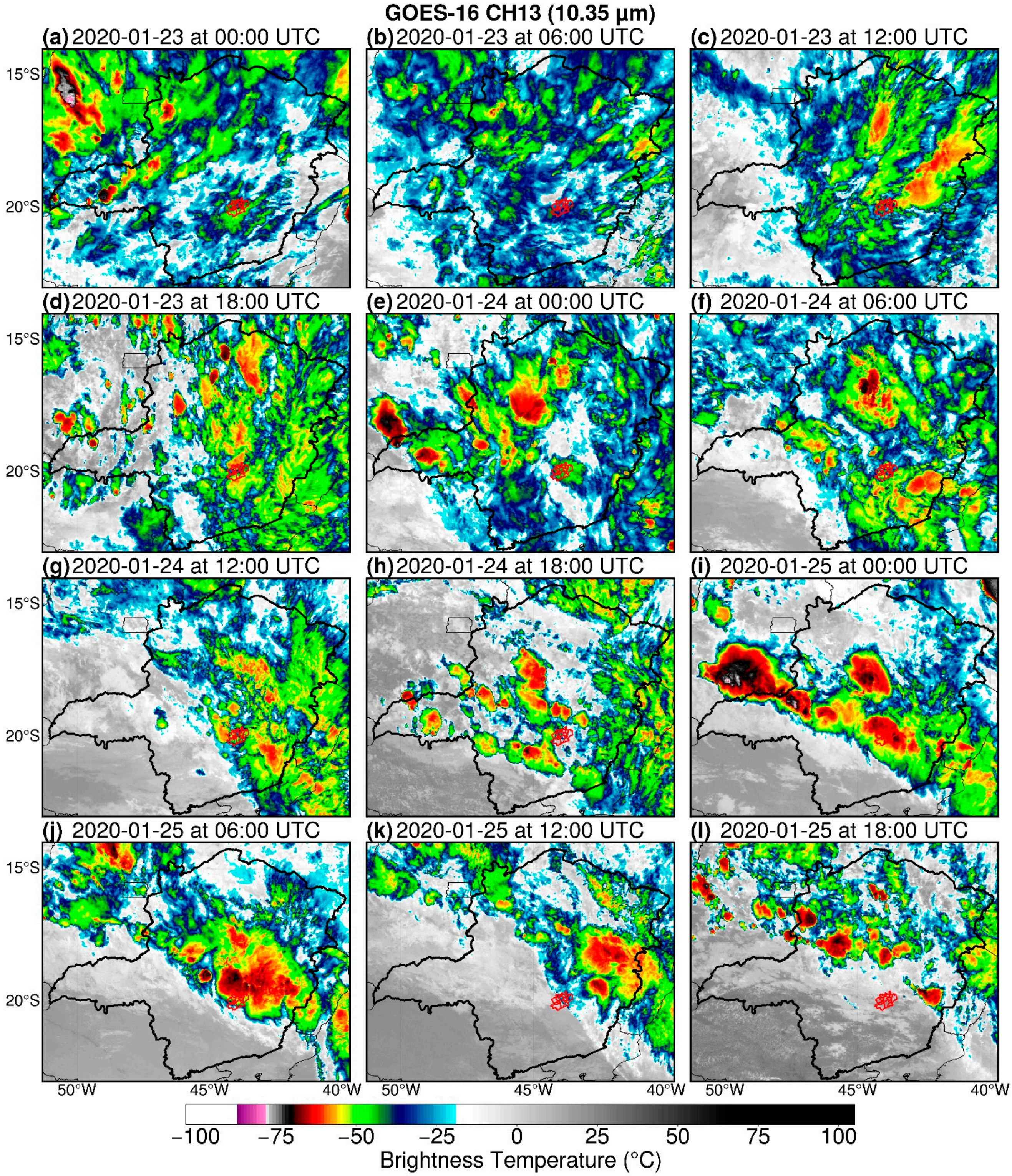


**Figure 12.** (**a**–**l**) Satellite images from GOES-16, channel 13 (10.3 µm) from 23 January 2020 at 00:00 UTC to 25 January 2020, at 18:00 UTC. The red line represents the MRBH.

Figure 13 illustrates the reflectivity observed by the radar at 3 km height from 23 January to 25 over the study region. A precipitating system developed from 23 to 12 UTC (09:00 local time) (Figure 13) and remained stationary over the area until 24 January, at 12:15 UTC (09:15 local time), dissipating at 18:12 UTC (15:12 local time). However, at 00:01 UTC (21:01 local time), a new system was formed over the MRBH and disbanded at noon UTC (09:00 local time) on the 25th. On the 24th, the convective cell persisted over the MRBH, indicating precipitation over the region, which coincides with data observed by rainfall stations (Figure 6). In Figure 14, it is possible to analyze the vertical structure of clouds over the MRBH. At that time, several precipitating cells were observed covering the radar area, and principally, more deep clouds occurred close to MRBH. For example, reflectivity values up to 40 dBZ were observed close to MRBH (Figure 14a). The vertical cross in this cloud indicates that its convective cell had a depth of approximately 5 km (Figure 14b). These results show that although at that moment the precipitating cell did not show very deep clouds with strong updrafts, it was the succession of clouds over several days that produced the high volume of accumulated rain in this region. This observation is consistent with the typical meteorological characteristics of SACZ.

Figure 15 shows the Minas Gerais state's lightning density for 23, 24, and 25 January. Note that on 24 January, the highest (up to four lightning strikes per day per $km^2$) lightning density occurred over the study region. This pattern agrees with what was discussed in Figure 12 about the spatial distribution of convective clouds. On 23 January, the convective cells were concentrated in the southwest of Minas Gerais, close to Goiás state. On 24 January, it concentrated in the MRBH, causing intense precipitation, as recorded by the rainfall stations (Figure 6), negatively impacting the region (Figure 5). Finally, on 25 January, there was less lightning density in the entire state of Minas Gerais. The relationship between convective clouds and the occurrence of lightning is justified because this type of cloud has a large vertical extension, favoring the formation of ice in its interior. As previously discussed, the wind shear in the region allowed for both the maintenance of rain clouds and the collision between the ice particles, allowing the electrification of the clouds and, consequently, lightning production [37]. However, for a better understanding of the lightning density of a storm, it is necessary to deepen the analysis regarding the cloud's growth rate, size, and temperature [38].

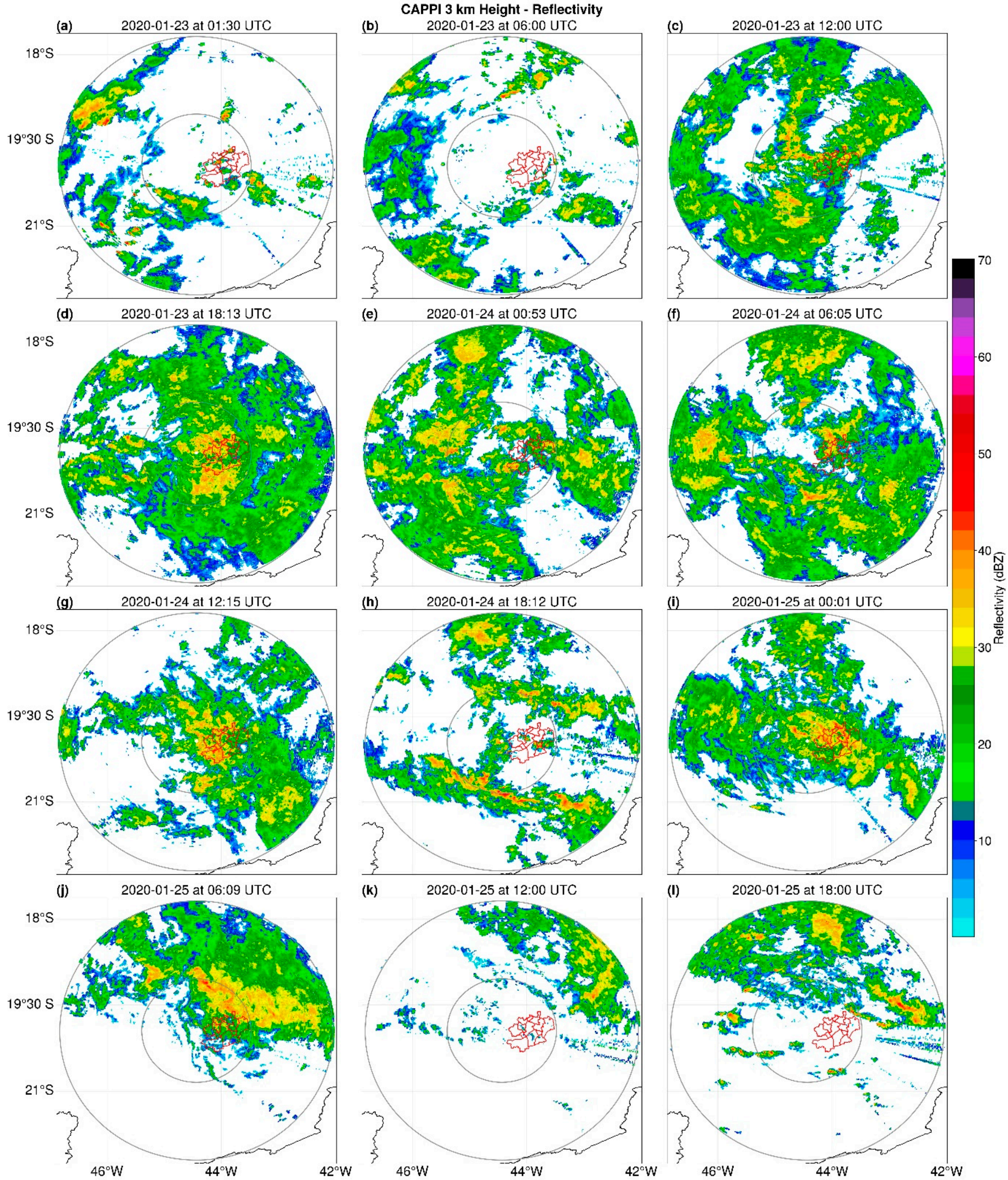


**Figure 13.** (**a**–**l**) Constant Plan Position Indication (CAPPI) of reflectivity at 3 km height from the weather radar, from 23 January 2020, at 01:30 UTC to 25 January 2020, at 18:00 UTC. The red line represents the MRBH.

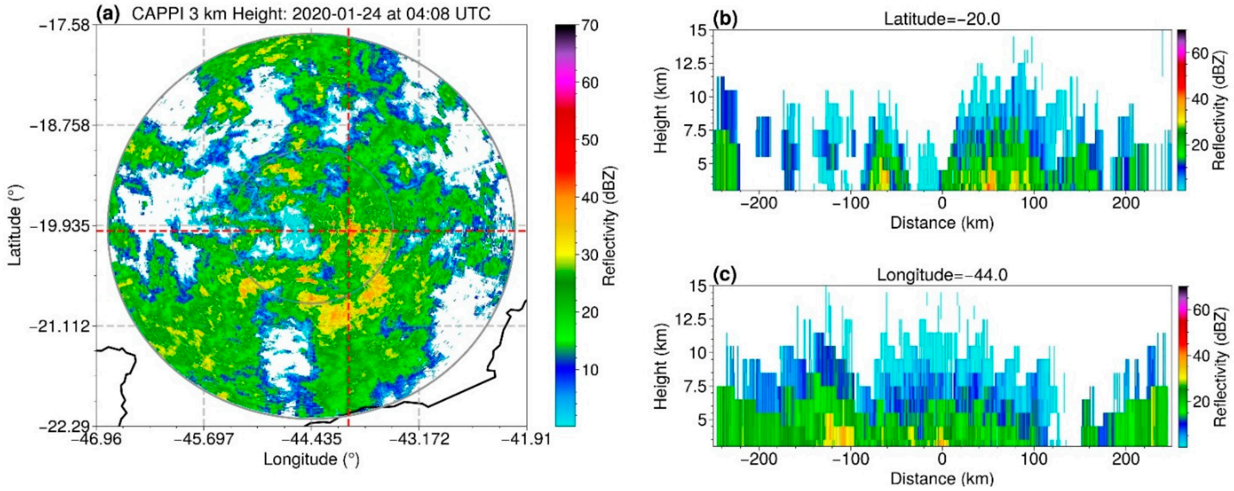


**Figure 14.** (**a**) CAPPI of reflectivity at 3 km height, and (**b**,**c**) vertical section of the thunderstorm in the MRBH on 24 January, at 04:08 UTC. The red lines in the CAPPI figures represent where the vertical sections were made.

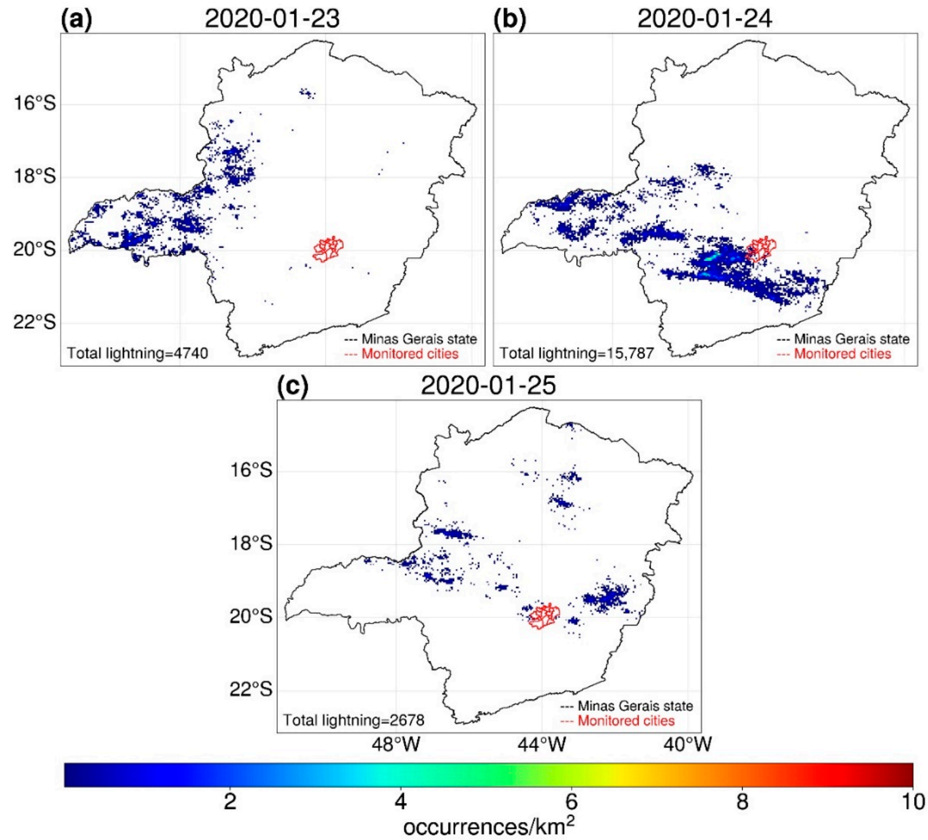


**Figure 15.** Spatial distribution of lightning density (intracloud plus cloud-to-ground in occurrences per day per km$^2$) of the Earth Networks Total Lightning Network for: (**a**) 23, (**b**) 24, and (**c**) 25 January 2020. The red line represents the MRBH.

## 4. Conclusions

This study evaluated the meteorological conditions that triggered the natural disasters in the MRBH between 23 and 25 January 2020. This event caused several inconveniences for the MRBH, harming more than 90 thousand people, resulting in economic losses of approximately USD 250 million and 13 deaths [12].

Thirty-two natural disasters in the MRBH were registered between 23 And 25 January 2020. Moderate precipitation (up to 150 mm $day^{-1}$) had been recorded since the beginning of the month, with a maximum of 240 mm $day^{-1}$ on 24 January. Throughout that same day, rainfall was recorded with a maximum of 48 mm $h^{-1}$. In addition, the increase in soil moisture since December 2023, reaching a maximum of 24 mm on 24 January, corroborates the occurrence of natural disasters. The extended duration of rainfall, combined with the region's soil characteristics, promoted substantial soil infiltration, which became saturated. These factors were pivotal for the occurrence and escalation of natural disasters.

Regarding the synoptic environment, the presence of the SACZ and the low-pressure system on the southeast coast of Brazil was responsible for the heavy rains that triggered floods and landslides in the study region. The mesoscale analysis through satellite images showed the occurrence of several clouds during the period of the natural disasters. Brightness temperatures as low as −65 °C were recorded for several convective cells.

Weather radar indicated that the thunderstorms presented precipitating cells throughout the study region, with moderate reflectivity (up to 40 dBZ). The spatial distribution of lightning density (intracloud plus cloud-to-ground) showed moderate intensity, with a peak of approximately four lightning strikes per day per $km^2$. Lightning indicates conditions favorable for ice formation and strong updrafts, essential for convective precipitation and lightning formation.

The meteorological analysis conducted in this study can contribute to understanding weather patterns associated with disasters in the MRBH. Other factors, not linked to natural phenomena but to socioeconomic conditions—such as the occupation of high-risk and vulnerable areas—are also relevant to the magnitude of these events. These factors are the main reasons for the number of people affected by natural disasters in Brazil.

In addition to enhancing scientific knowledge about meteorological patterns associated with natural disasters, the analysis presented in this work can also contribute to formulating and improving public policies aimed at disaster risk management in urban environments. This procedure can be applied to monitor and develop strategies for sustainable urban development. In Brazil, for example, the National Civil Defense and Protection Policy (PNPDEC) [39], instituted on 10 April 2012, aims to integrate prevention, mitigation, preparation, response, and recovery actions within the legal framework [39]. As observed by Oda et al. [19], the technical knowledge generated by such studies can help develop prevention, mitigation, and preparation strategies.

This study also highlights the importance of combining various meteorological datasets. To achieve this combination, expanding the network of meteorological stations and weather radars in Brazil is essential. Enhancing integration among meteorological centers would be a crucial step toward achieving this goal. For future work, considering climatological precipitation, it is suggested that the return period of such events for the state of Minas Gerais be evaluated. Additionally, studying vulnerability in this region, identifying risk areas, and jointly assessing the natural and social causes of the natural disasters recorded in this study are essential.

**Author Contributions:** Conceptualization, T.A.C.P., P.S.S.O., E.V.M. and D.O.d.S.; methodology, T.A.C.P., E.V.M., M.S.R., D.O.d.S., F.B.M. and T.S.B.; writing—original draft preparation, T.A.C.P. and P.S.S.O.; writing—review and editing, T.A.C.P., E.V.M., M.S.R., D.O.d.S., F.B.M., T.S.B. and G.W.d.S.F.; visualization, T.A.C.P. and P.S.S.O.; supervision, E.V.M. and D.O.d.S. All authors have read and agreed to the published version of the manuscript.

**Funding:** Financial support was received from the Minas Gerais Research Support Foundation (FAPEMIG) for granting scholarships to the first author (process number ID—11831), and the Coordination for the Improvement of Higher Education Personnel (CAPES, Finance Code 001) for providing the fifth author with master's scholarships. The third author also received support from the Brazilian National Council for Scientific and Technological Development (CNPq).

**Institutional Review Board Statement:** Not applicable.

**Informed Consent Statement:** Not applicable.

**Data Availability Statement:** The datasets used in this study are available from public online databases (links are provided in the Section 2).

**Conflicts of Interest:** The authors declare no conflicts of interest.

## References


1. WMO. World Meteorological Organization. The Atlas of Mortality and Economic Losses from Weather, Climate and Water Extremes (1970–2019). 2021. Available online: https://library.wmo.int/index.php?lvl=notice_display&id=21930#.YT_XuxmSlPZ (accessed on 23 September 2022).
2. IPCC. *Intergovernmental Panel on Climate Change, 2021*; Sixth Assessment Report (AR6). Climate Change 2021: The Physical Science Basis. Contribution of Working Group I to the Sixth Assessment Report of the Intergovernmental Panel on Climate Change; Cambridge University Press: Cambridge, UK, 2021.
3. Carvalho, D.; Damacena, F.A. Intensificação dos desastres naturais, as mudanças climáticas e o papel do Direito Ambiental. *Rev. Informação Legis* **2012**, *49*, 83–97. Available online: https://www2.senado.leg.br/bdsf/item/id/496559 (accessed on 22 December 2022).
4. Marengo, J.; Scarano, R.F.; Klein, F.A.; Souza, G.R.C.; Chou, C.S. Impacto, Vulnerabilidade e Adaptação das Cidades Costeiras Brasileiras às Mudanças Climáticas. Relatório Especial do Painel Brasileiro de Mudanças Climáticas (PBMC), 2016, 184. Available online: https://drive.google.com/file/d/1Bd0dOnFe6DLbDStm8eKI5oMK6LUHvURO/view (accessed on 16 November 2024).
5. Benini, R.M.; Mendiondo, E.M. Urbanização e impactos no ciclo hidrológico na Bacia do Mineirinho. *Floresta E Ambiente* **2015**, *22*, 211–222. [CrossRef]
6. UFSC. Universidade Federal de Santa Catarina. Universidade Federal de Santa Catarina. Atlas Brasileiro de Desastres Naturais—1991 a 2012: Minas Gerais, 2nd Ed., 2013. Florianópolis, Santa Catarina. Available online: https://educacao.cemaden.gov.br/midiateca/atlas-brasileiro-de-desastres-naturais-1991-a-2010/ (accessed on 16 November 2024).
7. Estadão, 2022. Minas Gerais é o Estado com Mais Desastres Naturais nos Últimos 10 Anos. Available online: https://www.em.com.br/app/noticia/gerais/2022/04/07/interna_gerais,1358442/minas-gerais-e-o-estado-com-mais-desastres-naturais-nos-ultimos-10-anos.shtml (accessed on 25 October 2022).
8. Reboita, M.S.; Rodrigues, M.; Silva, L.F.; Alves, M.A. Aspectos climáticos do estado de Minas Gerais. *Rev. Bras. Climatol.* **2015**, *17*, 206–226. [CrossRef]
9. Folha de São Paulo, 2003. Pior Enchente de Minas Gerais foi em 79. Available online: https://www1.folha.uol.com.br/folha/cotidiano/ult95u66816.shtml (accessed on 22 October 2022).
10. S2iD—Sistema Integrado de Informações Sobre Desastres Naturais. Série Histórica, 2016. Available online: https://s2id.mi.gov.br/paginas/series/ (accessed on 22 October 2022).
11. G1 Minas, 2020. Chuva Destrói Parte de BH; MG tem 55 Mortos em 6 Dias. Available online: https://g1.globo.com/mg/minas-gerais/noticia/2020/01/29/apos-mais-um-temporal-com-enchentes-bh-e-regiao-metropolitana-contabilizam-mais-estragos.ghtml (accessed on 22 October 2022).
12. Dalagnol, R.; Gramcianinov, C.; Crespo, N.; Luiz, R.; Chiquetto, J.; Marques, M.; Neto, G.; Abreu, R.; Li, S.; Lott, F.; et al. Extreme rainfall and its impacts in the Brazilian Minas Gerais state in January 2020: Can we blame climate change? *Clim. Resil. Sustain.* **2021**, *1*, e15. [CrossRef]
13. Kobiyama, M.; Mendonça, M.; Moreno, D.; Marcelino, I.; Marcelino, E.; Gonçalves, E.; Brazetti, L.; Goerl, R.; Molleri, G.; Rudorff, F. *Prevenção de Desastres Naturais Conceitos Básicos*, 1st ed.; Organic Trading: Curitiba, Brasil, 2006; pp. 1–124.
14. Gillespie, T.W.; Chu, J.; Frankenberg, E.; Thomas, D. Assessment and prediction of natural hazards from satellite imagery. *Prog. Phys. Geogr.* **2007**, *31*, 459–470. [CrossRef]
15. Rozante, J.R.; Moreira, D.S.; Gonçalves, L.G.G.; Vila, D. Combining TRMM and Surface Observations of Precipitation: Technique and Validation Over South America. *Weather Forecast.* **2010**, *25*, 885–894. [CrossRef]
16. Mecikalski, J.R.; Bedka, K.M. Forecasting convective initiation by monitoring the evolution of moving cumulus in daytime GOES imagery. *Mon. Weather Rev.* **2006**, *134*, 49–78. [CrossRef]
17. Freitas, A.A.; Oda, P.S.S.; Teixeira, D.L.S.; Silva, P.N.; Mattos, E.V.; Bastos, I.R.P.; Nery, T.D.; Metodiev, D.; Santos, A.P.P.; Gonçalves, W.A. Meteorological conditions and social impacts associated with natural disaster landslides in the Baixada Santista region from March 2nd–3rd, 2020. *Urban Clim.* **2022**, *42*, 1–22. [CrossRef]

18. Entekhabi, D.; Njoku, E.G.; O'neill, P.E.; Kellogg, K.H.; Crow, W.T.; Edelstein, W.N.; Entin, J.K.; Goodman, S.D.; Jackson, T.J.; Johnson, J.; et al. The Soil Moisture Active Passive (SMAP) Mission. In Proceedings of the IEEE; IEEE: Piscataway, NJ, USA, 2010; Volume 98, pp. 704–716. [CrossRef]
19. Oda, P.S.S.; Teixeira, D.L.S.; Pinto, T.A.C.; Silva, F.P.; Riondet-Costa, D.R.T.; Mattos, E.V.; Souza, D.O.; Bartolomei, F.; Reboita, M.S.; Santos, A.P.P. Disasters in Petrópolis, Brazil: Political, urban planning, and geometeorological factors that contributed to the event on 15 February 2022. *Urban Clim.* **2024**, *54*, 101849. [CrossRef]
20. Reboita, M.S.; Mattos, E.V.; Capucin, B.C.; Souza, D.O.; Ferreira, G.W.S. A multi-scale analysis of the extreme precipitation in southern Brazil in April/May 2024. *Atmosphere* **2024**, *15*, 1123. [CrossRef]
21. Buriol, T.M.; Beneti, C. Visualização científica interativa de dados de radar meteorológico. In *Proceeding Series of the Brazilian Society of Computational and Applied Mathematics*; CNMAC: Natal, Brasil, 2015; Volume 3. [CrossRef]
22. Abreu, E.X.; Mattos, E.V.; Sperling, V.B. Caracterização das assinaturas de radar e da atividade elétrica de relâmpagos de tempestades com granizo no estado de São Paulo. *Anuário Inst. Geociências* **2020**, *43*, 173–188. [CrossRef]
23. Soci, C.; Hersbach, H.; Simmons, A.; Poli, P.; Bell, B.; Berrisford, P.; Horányi, A.; Muñoz-Sabater, J.; Nicolas, J.; Radu, R.; et al. The ERA5 global reanalysis from 1940 to 2022. *Q. J. R. Meteorol. Soc.* **2024**, *150*, 4014–4048. [CrossRef]
24. Dee, D.P.; Uppala, S.M.; Simmons, A.J.; Berrisford, P.; Poli, P.; Kobayashi, S.; Andrae, U.; Balmaseda, M.A.; Balsamo, G.; Bauer, D.P.; et al. The ERA-Interim reanalysis: Configuration and performance of the data assimilation system. *Q. J. R. Meteorol. Soc.* **2011**, *137*, 553–597. [CrossRef]
25. Schultz, C.J.; Petersen, W.A.; Carey, L.D. Preliminary development and evaluation of lightning jump algorithms for the real-time detection of severe weather. *J. Appl. Meteorol. Climatol.* **2009**, *48*, 2543–2563. [CrossRef]
26. Parizzi, M.G.; Sebastião, C.S.; Viana, C.S.; Pflueger, M.C.; Campos, L.C.; Cajazeiro, J.M.D.; Tomich, R.S.; Guimarães, R.N.; Abreu, M.L.; Sobreira, F.G.; et al. Correlação entre chuvas e movimentos de massa no município de Belo Horizonte, MG. *Rev. Geogr.* **2010**, *6*, 49–68. [CrossRef]
27. Wiggers, M.M. Zoneamento das Áreas de Risco a Movimentos de Massa no Perímetro Urbano do Município de Caxias do Sul (RS). Master's Thesis, Federal University of Rio Grande do Sul, Porto Alegre, Brazil, 2013. Available online: https://lume.ufrgs.br/handle/10183/75687 (accessed on 22 October 2022).
28. Maffra, C.Q.T.; Centeno, J.A.S. Estimativa da umidade do solo por meio de sensoriamento remoto e suas possíveis aplicações no estudo de deslizamento de terra. *Rev. Bras. Cartogr.* **2016**, *68*, 1709–1719. [CrossRef]
29. Mendes, R.M.; Filho, M.V.; Santoro, J.; Faria, D.G.M.; Portela, V.D.A. Proposição de limiares críticos ambientais para uso em sistema de alertas de deslizamentos. *Rev. Dep. Geogr.* **2020**, *40*, 61–77. [CrossRef]
30. Barbosa, R.G. Variabilidade da Ocorrência de Deslizamentos de Terra e Sua Relação com a Precipitação na Cidade de Manaus. Master's Thesis, Amazonas State University, Manaus, Brazil, 2017. Available online: https://repositorio.inpa.gov.br/handle/1/12625 (accessed on 22 October 2022).
31. Silva, J.P.R.; Reboita, M.S.; Escobar, G.C.J. Caracterização da Zona de Convergência do Atlântico Sul em campos atmosféricos recentes. *Rev. Bras. Climatol.* **2019**, *25*, 355–377. [CrossRef]
32. Escobar, G.C.J.; Marques, A.C.D.A.; Dereczynski, C.P. Synoptic patterns of South Atlantic Convergence Zone episodes associated with heavy rainfall events in the city of Rio de Janeiro, Brazil. *Atmósfera* **2022**, *35*, 287–305. [CrossRef]
33. Carvalho, L.M.; Jones, C.; Liebmann, B. The South Atlantic convergence zone: Intensity, form, persistence, and relationships with intraseasonal to interannual activity and extreme rainfall. *J. Clim.* **2004**, *17*, 88–108. [CrossRef]
34. Joe, P.; Heizenreder, D.; Yeung, H.Y.; Dai, J.; Doi, K.; Suzuki, O.; Li, P.W.; James, P.; Lang, P.; Dance, S.; et al. Automated processing of doppler radar data for severe weather warnings. In *Doppler Radar Observations—Weather Radar, Wind Profiler, Ionospheric Radar, and Other Advanced Applications*; Bech, J., Chau, J.L., Eds.; IntechOpen: London, UK, 2012.
35. Rasmussen, E.; Blanchard, D.O. A baseline climatology of sounding-derived supercell and tornado forecast parameters. *Weather Forecast.* **1998**, *13*, 1148–1164. [CrossRef]
36. Nascimento, E.L. Previsão de tempestades severas utilizando-se parâmetros convectivos e modelos de mesoescala: Uma estratégia operacional adotável no Brasil? *Rev. Bras. Meteorol.* **2005**, *20*, 121–140.
37. Saunders, C.P.R. A review of thunderstorm electrification processes. *J. Appl. Meteorol. Climatol.* **1993**, *32*, 642–655. [CrossRef]
38. Monteiro, J.M.; Mattos, E.V.; Lima, W.F.A. Propriedades físicas e elétricas de tempestades na região Sudeste do Brasil. *Anuário Inst. Geociências* **2021**, *44*, 1–15. [CrossRef]
39. PNPDEC—Política Nacional de Proteção e Defesa Civil, Lei Federal nº 12.608, 2012. Available online: http://www.planalto.gov.br/ccivil_03/_Ato2011-2014/2012/Lei/L12608.htm (accessed on 22 December 2022).